Photophysical Properties of Pyrene-Functionalized Poly(propylene imine) Dendrimers

Lane A. Baker and Richard M. Crooks*

Department of Chemistry, Texas A&M University, P.O. Box 30012, College Station, Texas 77842-3012

Received August 7, 2000; Revised Manuscript Received October 3, 2000

ABSTRACT: Four generations of poly(propylene imine) dendrimers have been covalently modified with pyrene moieties and examined by fluorescence spectroscopy. Emission and excitation spectra were obtained so that the generational dependence of the dendrimers, especially the extent of steric crowding, could be correlated to the photophysical properties of pyrene. In particular, the effect of dendrimer concentration and generation on pyrene−pyrene interactions was evaluated. More excimer emission was observed for higher generation dendrimers, while little or no evidence for interdendrimer interactions was observed over more than 2 orders of magnitude in dendrimer concentration. Excitation spectra revealed the presence of preassociated pyrene moieties. Protonation of the tertiary amine units was shown to increase monomer fluorescence significantly, while only slightly increasing the observed excimer fluorescence.

Introduction

In this paper, we report the photophysical properties of poly(propylene imine) (PPI) dendrimers[1] modified on their periphery with fluorescent pyrene moieties. Specifically, derivatization of the primary amine end groups of generation 2, 3, 4, and 5 PPI dendrimers has been achieved via amidation with an activated pyrene derivative, yielding polymers peripherally modified with 8, 16, 32, and 64 pyrene moieties, respectively. The results indicate that the extent of interaction between terminal pyrene groups, which correlates to excimer fluorescence, is related to the generation-dependent dendrimer structure. Specifically, more excimer fluorescence arises from higher generation dendrimers that are more sterically crowded on their surfaces.

Dendrimers[2−8] are a class of highly symmetric (in some cases), monodisperse polymers that, relative to their linear analogues, possess a well-defined structure. A number of technological uses have been proposed for dendrimers,[3,5] and therefore a significant effort has been directed toward understanding their physical and chemical properties. Chromophore-labeled dendrimers, in particular, have proven to be an informative means for studying the properties of dendrimers.[9−23] Recent reports on the peripheral modification of dendrimers with moieties such as dansyl sulfonate,[24,25] porphyrins,[26] azobenzenes,[27] oligo(*p*-phenylene vinylenes),[28] and coumarin[29,30] moieties have shed new light on the structure and possible applications of dendrimers.

The fluorescent properties of pyrene are characterized by long lifetimes,[31] sensitive solvatochromic shifts,[32,33] and easily distinguished excimer species that arise when multiple pyrene molecules are π-stacked or in close proximity.[31] For these reasons, pyrene is an obvious candidate to exploit in the study of polymer structure and function. For example, previous studies have shown that pyrene can be used to probe structure and both intermolecular[34] and intramolecular interactions for a variety of polymers, notably (hydroxypropyl)cellulose[35−38] and poly(ethylene imine),[39−41] a polymer closely related to the PPI dendrimers in this study.

* To whom correspondence should be addressed. e-mail crooks@tamu.edu; fax 979-845-1399; phone 979-845-5629.

Recent studies by Paleos et al. have focused on the properties of pyrene noncovalently trapped within poly(amido amine) (PAMAM)[42] and PPI dendrimers.[43,44] These reports have shown that pyrene can be sequestered in the interior cavity of dendrimers and selectively released by protonating interior tertiary amines at the branch points. This is a consequence of the hydrophobic nature of pyrene and the enhanced hydrophilicity of the dendrimer interior upon protonation. Fox and co-workers have modified polyether dendrons with pyrene and naphthalene and examined the energy transfer properties between the core and these terminal groups.[45] Dendrimers having aryl[46] and carbosilane[47,48] backbones covalently modified with pyrene have been studied by Adams and Vitukhnovsky, respectively. Adams et al. selectively modified each dendron of several different generation dendrimers with one pyrene moiety (three pyrene moieties per dendrimer independent of generation) and studied these molecules with time-resolved fluorescence techniques. They observed increased mobility in the end groups from generation one to three by monitoring the magnitude of the excimer and monomer fluorescence bands. Vitukhnovsky modified the core of the dendrimer with a single pyrene moiety and used time-resolved and polarized fluorescence techniques to correlate the reorientation times of pyrene to the dendrimer structure. Moore and Kopelman have studied excimer formation and energy migration in phenylacetylene dendrimers having perylene traps.[49]

In this paper, we describe the functionalization and spectroscopic properties of four generations of PPI dendrimers fully substituted with pyrene. The results indicate that the excimer-to-monomer fluorescence ratio increases as dendrimer generation increases. Additionally, fluorescence excitation spectra confirm the presence of preaggregated pyrene moieties. Spectra obtained at low pH indicate that monomer fluorescence is quenched by protonated tertiary amines present in the dendrimer backbone more strongly than excimer fluorescence resulting from aggregated pyrene. Supporting evidence for the generational dependence of dendrimer generation on the fluorescent properties is provided by molecular dynamics (MD) simulations. On the basis of the results described in this paper, we propose that

10.1021/ma001379c CCC: $19.00
Published on Web 11/03/2000

functional groups attached to dendrimer surfaces at high density can interact with one another and thereby exhibit new functions. Such "cooperative effects" are closely related to the "proximity effect" demonstrated here and might have practical applications for sensing and catalysis. Similar observations have been made for other multifunctional molecules, such as cyclodextrins,[50−52] cryptands,[53] and linear and hyperbranched polymers.[54−56] Dendrimers are an especially intriguing scaffold for controlling cooperativity between functional groups because the average spacing between moieties can be controlled by varying the dendrimer generation and the length of spacer groups separating the active functional group from the dendrimer itself. Moreover, the number of active functional groups can be controlled over a very wide range, which is limited only by the maximum dendrimer generation that can be synthesized.

Experimental Section

Chemicals. Second through fifth generation amine-terminated poly(propylene imine) dendrimers (PPI−$(NH_2)_X$) (X = 8, 16, 32, and 64 for generations 2, 3, 4, and 5, respectively) were used as received (DSM Fine Chemicals, The Netherlands). 1-Pyrenebutyric acid *N*-hydroxysuccinimide ester (Aldrich 97%), anhydrous dichloromethane (Aldrich 99.8%), and sulfuric acid (EM Scientific) were also used as received. Triethylamine (Aldrich 99%) was stored over molecular sieves (Aldrich, 3 Å) prior to use. Spectroscopic grade *N*,*N*-dimethylformamide (Acros 99+%) was used to prepare solutions for all spectroscopic measurements.

Procedures. Dendrimers were functionalized by dissolving (separately) PPI−$(NH_2)_8$ (84.5 mg = 0.109 mmol), PPI−$(NH_2)_{16}$ (84.9 mg = 0.0503 mmol), PPI−$(NH_2)_{32}$ (89.4 mg = 0.0254 mmol), or PPI−$(NH_2)_{64}$ (147.0 mg = 0.0205 mmol) in 10 mL of dry dichloromethane containing 0.2 mL of dry triethylamine. Sufficient pyrenebutyric acid *N*-hydroxysuccinimide ester dissolved in 2 mL of dry dichloromethane was added to each dendrimer solution to yield a 30% excess relative to the number of terminal amine groups of the dendrimers. After stirring for 48 h, ninhydrin tests of the reaction mixture indicated complete functionalization of the primary amines of the dendrimers. Each solution of functionalized dendrimer (PPI−Py_X, where X = 8, 16, 32, or 64) was then washed three times with saturated aqueous NaCl, saturated aqueous Na_2CO_3, and 0.1 M HCl, followed by repetitive reprecipitations from chloroform/hexane and chloroform/diethyl ether. Transmission IR, ^{1}H NMR, and ^{13}C NMR of the PPI−Py_X dendrimers confirm 100% functionalization of the dendrimer peripheries. Percent yields (calculated based on 100% functionalization) are given below. MALDI-TOF data for PPI−Py_8 and PPI−Py_{16} are also provided.

PPI−Py_8 (75.1 mg, 25% yield). ^{1}H NMR (200 MHz, CD_2Cl_2): δ 1.40 (28H br, $NCH_2CH_2CH_2N$, $NCH_2CH_2CH_2NH$, $NCH_2CH_2CH_2CH_2N$), 2.18 (68H br, $N(CH_2)_3$, $COCH_2$, $COCH_2CH_2$), 3.12 (32H br, CH_2NH, $PyCH_2$), 6.85 (8H br, NH), 7.50−8.30 (72H m, Py). ^{13}C NMR (500 MHz, $CDCl_3$): δ 27.1 ($NCH_2CH_2CH_2NHCO$), 27.8 ($COCH_2CH_2CH_2$), 33.0 (CH_2Py), 36.2 (CH_2CH_2CO), 38.1 (CH_2CH_2NHCO), 51−53 ($N(CH_2)_3$), 123−136 (Py), 173.2 (CO). IR (NaCl plates): amide I 1650 cm^{-1}, amide II 1540 cm^{-1}. MS (MALDI-TOF) calculated for $C_{200}H_{208}N_{14}O_8$: 2936; found 2958 $[M + Na]^+$.

PPI−Py_{16} (35.2 mg, 12% yield). ^{1}H NMR (200 MHz, CD_2Cl_2): δ 1.39 (60H br, $NCH_2CH_2CH_2N$, $NCH_2CH_2CH_2NH$, $NCH_2CH_2CH_2CH_2N$), 2.14 (148H br, $N(CH_2)_3$, $COCH_2$, $COCH_2CH_2$), 3.12 (64H br, CH_2NH, $PyCH_2$), 7.05 (16H br, NH), 7.40−8.30 (144H m, Py). ^{13}C NMR (500 MHz, $CDCl_3$): δ 24.6 ($NCH_2CH_2CH_2CH_2N$, $NCH_2CH_2CH_2N$), 27.1 ($NCH_2CH_2CH_2NHCO$), 27.8 ($COCH_2CH_2CH_2$), 33.0 (CH_2Py), 36.2 (CH_2CH_2CO), 38.0 (CH_2CH_2NHCO), 51−53 ($N(CH_2)_3$), 123−136 (Py), 173.2 (CO). IR (NaCl plates): amide I 1650 cm^{-1}, amide II 1540 cm^{-1}. MS (MALDI-TOF) calculated for $C_{408}H_{432}N_{30}O_{16}$: 6012; found 6038 $[M + Na]^+$.

PPI−Py_{32} (48.6 mg, 16% yield). ^{1}H NMR (200 MHz, CD_2Cl_2): δ 1.35 (124H br, $NCH_2CH_2CH_2N$, $NCH_2CH_2CH_2NH$, $NCH_2CH_2CH_2CH_2N$), 2.12 (308H br, $N(CH_2)_3$, $COCH_2$, $COCH_2CH_2$), 3.05 (128H br, CH_2NH, $PyCH_2$), 7.20 (32H br, NH), 7.35−8.30 (576H m, Py). ^{13}C NMR (500 MHz, $CDCl_3$): δ 24.6 ($NCH_2CH_2CH_2CH_2N$, $NCH_2CH_2CH_2N$), 27.2 ($NCH_2CH_2CH_2NHCO$), 27.8 ($COCH_2CH_2CH_2$), 33.0 (CH_2Py), 36.2 (CH_2CH_2CO), 38.0 (CH_2CH_2NHCO), 51−53 ($N(CH_2)_3$), 123−136 (Py), 173.3 (CO). IR (NaCl plates): amide I 1641 cm^{-1}, amide II 1541 cm^{-1}.

PPI−Py64 (161.7 mg, 32% yield). ^{1}H NMR (200 MHz, CD_2Cl_2): δ 1.35 (252H br, $NCH_2CH_2CH_2N$, $NCH_2CH_2CH_2NH$, $NCH_2CH_2CH_2CH_2N$), 2.10 (628H br, $N(CH_2)_3$, $COCH_2$, $COCH_2CH_2$), 3.02 (256H br, CH_2NH, $PyCH_2$), 7.10−8.30 (640H br, NH, Py). ^{13}C NMR (500 MHz, $CDCl_3$): δ 24.7 ($NCH_2CH_2CH_2CH_2N$, $NCH_2CH_2CH_2N$), 27.2 ($NCH_2CH_2CH_2NHCO$), 27.8 ($COCH_2CH_2CH_2$), 32.9 (CH_2Py), 36.1 (CH_2CH_2CO), 37.9 (CH_2CH_2NHCO), 51−53 ($N(CH_2)_3$), 123−136 (Py), 173.4 (CO). IR (NaCl plates): amide I 1643 cm^{-1}, amide II 1538 cm^{-1}.

Molecular Modeling. Modeling was performed in a manner analogous to previous reports in the literature.[57−60] Molecular models were created using the Cerius^2 (version 4.0) software package (Molecular Simulations, Inc.; San Diego, CA). The DREIDING force field[61] version 2.21 was used for optimization and molecular dynamics simulations. Specifically, each generation of PPI dendrimers was constructed from a model of the previous generation by adding the appropriate number of propylamine branches. The SMART algorithm and standard convergence settings were used to energy minimize each generation. Molecular dynamics (MD) simulations were then performed by the NVT method (constant volume and temperature) using the Nosé temperature thermostat (0.01 ps relaxation) for 10 ps at 1000 K, followed by 250 ps at 300 K with a step size of 1 fs. The structures were again energy minimized. After obtaining models of each generation, all primary amines were functionalized with pyrenebutyric acid groups, thereby creating models of the dendrimers of interest. Minimization and dynamics were performed again, exactly as described for the unmodified dendrimers. Static properties reported are calculated based on the final minimized structure. Dynamic properties reported are calculated on the basis of the last 50 ps of dynamics simulation, for which equilibrium had been reached.

Fluorescence Measurements. Fluorescence measurements were carried out at 22 °C using an SLM-AMINCO spectrometer (Spectronic Unicam; Rochester, NY) equipped with excitation and emission monochromators and a water-cooled sample stage. Emission slits were set at 2 nm. The excitation wavelength was 345 nm. Excitation spectra were monitored at 377 and 476 nm respectively for monomer and excimer spectra. Spectra were corrected for solvent scattering by subtraction of an appropriate blank solution.

Results and Discussion

Molecular Models. Molecular simulations are useful for assessing both the flexibility of the dendrimer backbone and the possible proximity of appended moieties. Accordingly, molecular models were grown in a divergent manner for generation 2−5 amine-terminated PPI dendrimers. Each optimized generation was then functionalized with pyrene butyric acid, thereby mimicking the synthetic procedure used to prepare the authentic materials (Figure 1). Radii of gyration derived from optimized PPI−$(NH_2)_x$ dendrimers indicate that these models provide results consistent with previous theoretical and experimental values reported by Scherrenberg et al.[58] for amine-terminated dendrimers (Table 1). The total energy per atom and van der Waals energy (steric energy) changes very little as a function of generation for both amine- and pyrene-terminated dendrimers, which is also consistent with previous modeling studies by Cavallo and Fraternali on phenylalanine-modified PPI dendrimers.[57]

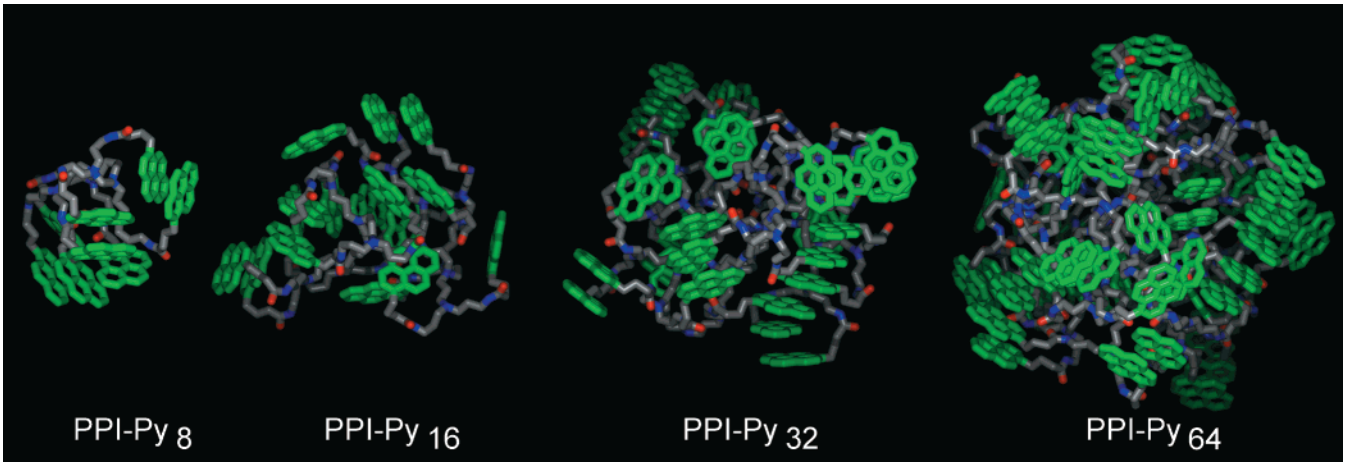

Figure 1. Molecular models of (left to right) PPI−Py_8, PPI−Py_{16}, PPI−Py_{32}, and PPI−Py_{64} dendrimers (pyrenyl carbons, green; nitrogen, blue; oxygen, red; and dendrimer carbons, gray). The hydrogens are omitted for clarity.

Table 1. Properties of Amine- and Pyrene-Teminated PPI Dendrimers Derived from Molecular Simulations; Values Are Calculated Using the DREIDING Force Field

	PPI−$(NH_2)_8$	PPI−$(NH_2)_{16}$	PPI−$(NH_2)_{32}$	PPI−$(NH_2)_{64}$	PPI−Py_8	PPI−Py_{16}	PPI−Py_{32}	PPI−Py_{64}
no. of atoms	150	326	678	1382	430	886	1798	3622
mol wt (g/mol)	773	1687	3514	7168	2935	6012	12165	24469
radius of gyration (Å)	6.77	8.23	9.70	13.00	8.54	10.80	13.84	17.00
total energy (kcal/mol)	129.40	277.77	543.30	1104.00	403.10	894.70	1968.00	4039.00
total energy per atom (kcal/mol)	0.86	0.85	0.80	0.80	0.94	1.01	1.09	1.12
VDW energy (kcal/mol)[a]	67.51	131.01	226.78	575.65	329.80	628.15	1148.96	2359.00
VDW energy per atom (kcal/mol)	0.45	0.40	0.33	0.42	0.77	0.71	0.64	0.65

[a] VDW = van der Waals.

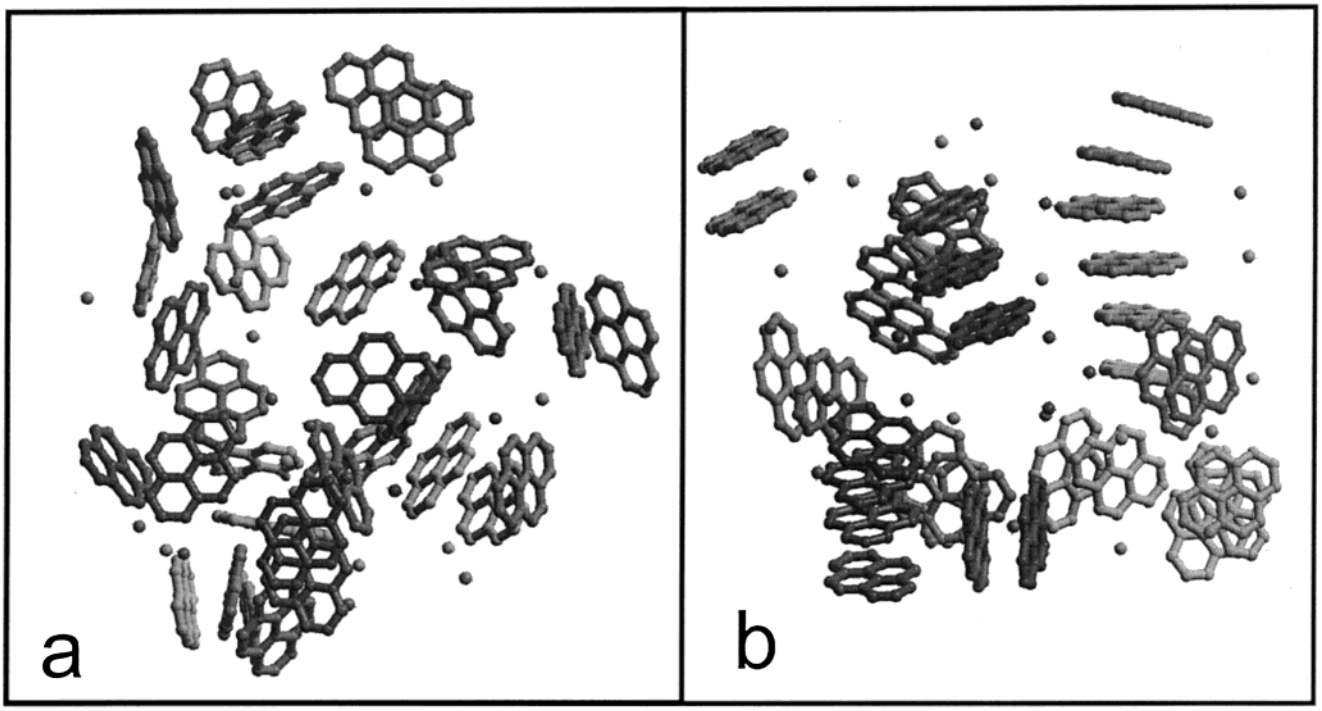

Figure 2. Distribution and ordering of sp^2 carbon atoms (aromatic pyrene and amide carbonyl) in PPI−Py_{32} (a) prior to molecular dynamics run and (b) after molecular dynamics run.

Figure 2 shows all sp^2-hybridized carbon atoms (pyrene and amide carbonyl) in energy-minimized PPI−Py_{32} models before and after the MD run. Significant reordering of the dendritic framework to allow for π-stacking of the pyrene moieties is obvious. In the case of PPI−Py_8 and PPI−Py_{16}, the pyrene moieties are able to wrap completely around the dendrimer, resulting in a single, aggregated clump of pyrene molecules. However, due to the size of PPI−Py_{32} and PPI−Py_{64}, and the resulting steric congestion on the surface of these materials, the lowest-energy structures are those forming smaller pyrene aggregates.

Characterization and Spectroscopic Measurements. Nearly 100% pyrene functionalization of the PPI

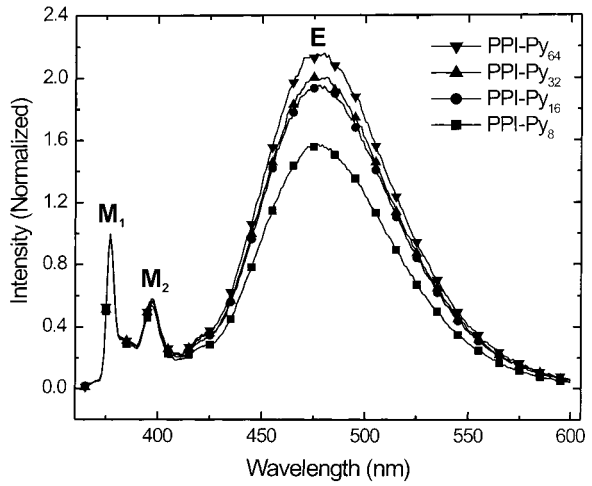

Figure 3. Emission spectra of PPI−Py_8, PPI−Py_{16}, PPI−Py_{32}, and PPI−Py_{64} pyrene-terminated dendrimers. The spectra were normalized at 377 nm, obtained in DMF, and $\lambda_{exc} = 345$ nm. Peaks present at 377 nm (M_1) and 398 nm (M_2) arise from monomer fluorescence and the broad peak at 476 nm (E) arises from excimer emission.

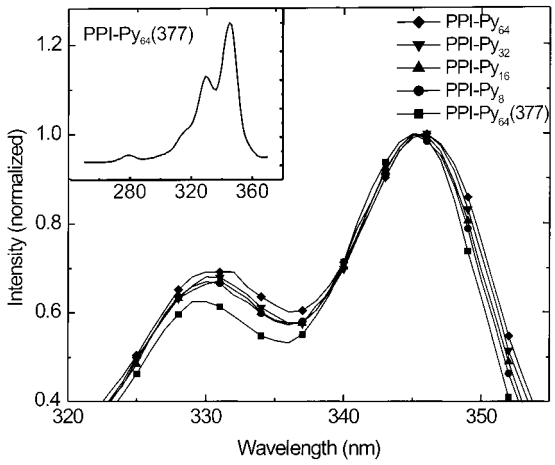

Figure 4. Normalized excitation spectra for PPI−Py_8, PPI−Py_{16}, PPI−Py_{32}, and PPI−Py_{64} monitored at the excimer emission wavelength (476 nm). Excitation spectra recorded at the monomer emission wavelength (377 nm) were identical to one another, and an example is also shown in the figure for PPI−Py_{64}. The inset shows the full spectral region examined for PPI−Py_{64} (excitation monitored at 377 nm).

periphery is required for meaningful interpretation of our results and for comparison to the just-described MD simulations. As discussed in the Experimental Section, the synthetic chemistry required to prepare these materials is relatively straightforward and proceeds with yields of up to 30%. Purification by repetitive reprecipitations is time-consuming and results in significant loss of product (particularly from diethyl ether) but does provide pure material. Ninhydrin tests spotted on TLC plates of the reaction mixture showed no indication of unreacted primary amines. ^{1}H NMR is informative for verifying coupling between the dendrimer and pyrene moiety, because a peak corresponding to bond formation arises from the amide proton. As previously reported, this peak shifts downfield with increasing dendrimer generation because of enhanced intramolecular hydrogen bonding in these more sterically crowded materials.[62] ^{1}H NMR also indicates the absence of residual starting materials. Confirmation of complete amidation of primary amines is observed in the ^{13}C NMR by a shift from ca. 40 to ca. 38 ppm of the carbon at the position α to the newly created amide bond, in good agreement with previous literature reports.[63−65] Additionally, the lone carbonyl signal arising from the amide at ca. 173 ppm indicates the absence of residual starting materials. MALDI-TOF spectra for PPI−Py_8 and PPI−Py_{16} reveal M−Na^+ ions but no evidence of dendrimers missing one or more pyrene groups (see Supporting Information). These findings confirm quantitative functionalization of the dendrimers with pyrene. We were unable to obtain meaningful MALDI-TOF data for PPI−PY_{32} and PPI−Py_{64}.

PPI dendrimers functionalized with pyrene afford a convenient means for studying intramolecular terminal-group interactions using fluorescence spectroscopy. Figure 3 presents fluorescence emission spectra, normalized to the intensity at 377 nm, for four generations of pyrene-modified dendrimers in dimethylformamide (DMF).[66] Peaks due to monomeric pyrene emission are evident at 377 and 398 nm (labeled M_1 and M_2, respectively, in the figure), and a broad excimer emission is centered at 476 nm (labeled E in the figure). The excimer fluorescence arises from the close proximity of pyrene functional groups on individual dendrimers. As suggested by the previously described modeling studies, these results indicate that the pyrene groups are in electronic communication with one another.

Dilutions over 2 orders of magnitude (10^{-6}−10^{-8} M) demonstrate that the excimer-to-monomer ratio (I_E/I_{M1}) is independent of dendrimer concentration (see Supporting Information). This indicates that intermolecular processes do not play a significant role in excimer formation but rather arise principally from intradendrimer processes. The I_E/I_{M1} peak height ratio for PPI−Py_{64} is highest, followed by PPI−Py_{32} and PPI−Py_{16}, which have similar ratios, and finally by PPI−Py_8, which has the lowest I_E/I_{M1} ratio (see Supporting Information). For example, considering dendrimer solutions that contain a nominal pyrene concentration of 1.5×10^{-6} M, the I_E/I_{M1} ratios are 1.56, 1.95, 1.99, and 2.19 for PPI−Py_8, PPI−Py_{16}, PPI−Py_{32}, and PPI−Py_{64}, respectively. We suggest that this increase is correlated to the increase in the density of pyrene groups on the dendrimer periphery as a function of generation. Specifically, the surface density of terminal amine groups on these dendrimers ranges from 1.4 NH_2 groups/nm^2 for PPI−$(NH_2)_8$ to 3.0 NH_2 groups/nm^2 for PPI−$(NH_2)_{64}$. On the basis of their larger diameter, the corresponding surface densities for the pyrene-functionalized dendrimers range from 0.9 Py groups/nm^2 for PPI−Py_8 to 1.8 Py groups/nm^2 for PPI−Py_{64}.[67]

In addition to dynamic excimers, it is well-established that pyrene can form ground-state dimers, or so-called "static excimers".[31] The existence of such dimers can be probed using excitation spectra.[38] Excitation spectra monitored at the monomer emission wavelength (377 nm) were similar for all PPI−Py_n generations. By way of example, the monomer excitation spectrum for PPI−Py_{64} is shown over the entire wavelength range studied in the inset of Figure 4; a more detailed view is shown in the main body of the figure. Excitation spectra monitored at the excimer emission wavelength (476 nm) for all dendrimer generations are also shown in Figure 4. Two facts are clearly evident by inspection of the excimer excitation spectrum. First, there is a slight red shift with increasing dendrimer generation in the peak near 345 nm. The magnitude of this shift (1−2 nm) is in accord with that previously reported for aggregated,

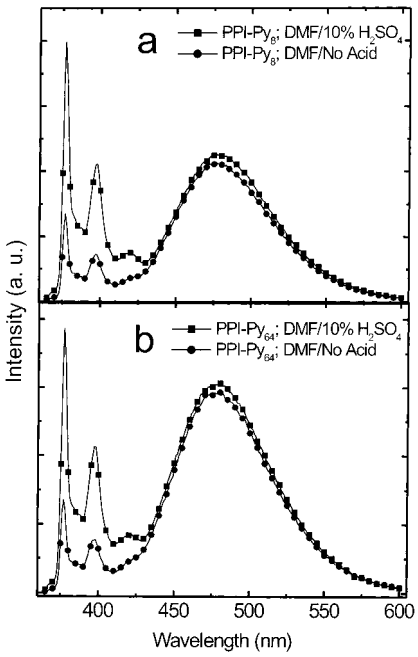

Figure 5. Fluorescence emission spectra of (a) PPI−Py_8 in DMF and in DMF/10 vol % H_2SO_4 and (b) PPI−Py_{64} in DMF and in DMF/10 vol % H_2SO_4. The data are not corrected for the 10% dilution caused by addition of the acid.

ground-state pyrene moieties present in solutions of pyrene-modified (hydroxypropyl)cellulose[35−38] and poly(ethylene imine).[39] Second, there is a decrease in the ratio of the peak height at 345 nm to the valley height at 336 nm. This indicates that the peaks become broader with increasing generation as a result of more aggregated pyrene molecules.[39] It should be noted, however, that excitation spectra cannot be used to distinguish between intra- and interdendrimer pyrene aggregates, nor can excitation spectra be used to determine sizes of the aggregates. Because aggregated pyrene was observed at all concentrations and for all generations studied, however, we expect they arise from intramolecular processes.

Thus far we have discussed interactions between pyrene terminal groups, but it is also interesting from a structural perspective to consider interactions between the pyrene terminal groups and the dendrimer branches. Pyrene is a good probe of such interactions, because tertiary amines (much more so than secondary or primary amines) have previously been shown to effectively quench monomeric pyrene fluorescence.[39,68] For example, the interior branch points of PPI dendrimers are tertiary amines, which have previously been demonstrated to quench the fluorescence of free pyrene contained within PPI dendrimers[14,42,44] and to quench fluorescence from pyrene covalently attached to the exterior of hyperbranched poly(ethylene imine).[39] In the case of pyrene-modified dendrimers, changing the apparent pH of the solution by the addition of acid allows the interaction between the dendrimer backbone and pendant pyrene groups to be examined. (It has been shown that protonation prevents quenching by the tertiary amines, presumably by tying up the nitrogen lone pair of electrons.[39,68]) Figure 5 shows the effect of the addition of H_2SO_4 (10 vol % final solution concentration) on the tertiary amines and the resulting fluorescence emission spectra for PPI−Py_8 and PPI−Py_{64}. Very little change is observed in the excimer fluorescence, while the monomer fluorescence increases for both generations.[69] From these results we conclude that unprotonated tertiary amines present in the dendrimer backbone selectively quench monomeric pyrene fluorescence. Furthermore, pyrene, and possibly other terminal-group modifiers, exhibit substantial interactions with the tertiary amines present in the backbone of PPI dendrimers. This finding may be applicable to the use of dendrimers as catalysts or chemical sensors.

Summary and Conclusions

We have examined the fluorescence arising from four generations of pyrene-terminated PPI dendrimers in DMF. Three trends are clearly evident. First, as dendrimer generation increases, so does the excimer-to-monomer ratio for pyrene emission. That is, with increasing generation the pyrene molecules are increasingly aggregated on the dendrimer periphery in such a way that excimer formation is enhanced. Second, interactions between the pyrene moieties prior to excitation (preaggregation) is present, as shown by the excitation spectra. Third, interactions between the pyrene pendant groups and the dendrimer backbone is also evident on the basis of the relative quenching as a function of pH. Specifically, protonation of the dendrimer gives rise to enhanced monomer emission.

We envision that the ability to tailor the proximity and interaction of functional groups by grafting moieties to the terminal groups of dendrimers will result in innovative applications for these unique polymers. In future studies we plan to exploit such interactions for catalysis and sensing applications.

Acknowledgment. The authors gratefully acknowledge the National Science Foundation (CHE-9818302) and the American Chemical Society Petroleum Research Fund (ACS-PRF#35756) for financial support. We thank Dr. Li Sun for insightful discussions. We also thank Dr. Lisa M. Thomson and the Texas A&M Laboratory for Molecular Simulation for assistance with calculations and the use of software and computing time.

Supporting Information Available: ^1H NMR and dependence of the monomer-to-excimer fluorescence ratio on dendrimer concentration for all generations, and MALDI-TOF for PPI−Py_8 and PPI−Py_{16}. This material is available free of charge via the Internet at http://pubs.acs.org.

References and Notes

(1) de Brabander-van den Berg, E. M. M.; Meijer, E. W. *Angew. Chem., Int. Ed. Engl.* **1993**, *32*, 1308−1311.
(2) Smith, D. K.; Diederich, F. *Chem. Eur. J.* **1998**, *4*, 1353−1361.
(3) Bosman, A. W.; Janssen, H. M.; Meijer, E. W. *Chem. Rev.* **1999**, *99*, 1665−1688.
(4) Dvornic, P. R.; Tomalia, D. A. *Macromol. Symp.* **1994**, *88*, 123−148.
(5) Fischer, M.; Vögtle, F. *Angew. Chem., Int. Ed. Engl.* **1999**, *38*, 4000−4021.
(6) Issberner, J.; Moors, R.; Vögtle, F. *Angew. Chem., Int. Ed. Engl.* **1994**, *33*, 2413−2420.
(7) Tomalia, D. A.; Naylor, A. M.; Goddard, W. A. *Angew. Chem., Int. Ed. Engl.* **1990**, *29*, 138−175.
(8) Zeng, F.; Zimmerman, S. C. *Chem. Rev.* **1997**, *97*, 1681−1712.
(9) Balzani, V.; Campagna, S.; Denti, G.; Juris, A.; Serroni, S.; Venturi, M. *Acc. Chem. Res.* **1998**, *31*, 26−34.
(10) ben-Avraham, D.; Schulman, L. S.; Bossman, S. H.; Turro, C.; Turro, N. J. *J. Phys. Chem. B* **1998**, *102*, 5088−5093.
(11) Bo, Z.; Zhang, W.; Zhang, X.; Zhang, C.; Shen, J. *Macromol. Chem. Phys.* **1998**, *199*, 1323−1327.
(12) Cardona, C. M.; Alvarez, J.; Kaifer, A. E.; McCarley, T. D.; Pandey, S.; Baker, G. A.; Bonzagni, N. J.; Bright, F. V. *J. Am. Chem. Soc.* **2000**, *122*, 6139−6144.

(13) Devadoss, C.; Bharathi, P.; Moore, J. S. *J. Am. Chem. Soc.* **1996**, *118*, 9635−9644.
(14) Gopidas, K. R.; Leheny, A. R.; Caminati, G.; Turro, N. J.; Tomalia, D. A. *J. Am. Chem. Soc.* **1991**, *113*, 7335−7342.
(15) Jockusch, S.; Turro, N. J.; Tomalia, D. A. *Macromolecules* **1995**, *28*, 7416−7418.
(16) Jockusch, S.; Turro, N. J.; Tomalia, D. A. *J. Inf. Recording* **1996**, *22*, 427−433.
(17) Jockusch, S.; Ramirez, J.; Sanghvi, K.; Nociti, R.; Turro, N. J.; Tomalia, D. A. *Macromolecules* **1999**, *32*, 4419−4423.
(18) Junge, D. M.; McGrath, D. V. *Chem. Commun.* **1997**, 857−858.
(19) Newkome, G. R.; Narayanan, V. V.; Godínez, L. A.; Pérez-Cordero, E.; Echegoyen, L. *Macromolecules* **1999**, *32*, 6782−6791.
(20) Plevoets, M.; Vögtle, F.; De Cola, L.; Balzani, V. *New J. Chem.* **1999**, 63−69.
(21) Tabakovic, I.; Miller, L. L.; Duan, R. G.; Tully, D. C.; Tomalia, D. A. *Chem. Mater.* **1997**, *9*, 736−745.
(22) Thornton, A.; Bloor, D.; Cross, G. H.; Szablewski, M. *Macromolecules* **1997**, *30*, 7600−7603.
(23) Yokoyama, S.; Nakahama, T.; Otomo, A.; Mashiko, S. *J. Am. Chem. Soc.* **2000**, *122*, 3174−3181.
(24) Balzani, V.; Ceroni, P.; Gestermann, S.; Kauffmann, C.; Gorka, M.; Vögtle, F. *Chem. Commun.* **2000**, 853−854.
(25) Vögtle, F.; Gestermann, S.; Kauffmann, C.; Ceroni, P.; Vicinelli, V.; De Cola, L.; Balzani, V. *J. Am. Chem. Soc.* **1999**, *121*, 12161−12166.
(26) Yeow, E. K. L.; Ghiggino, K. P.; Reek, J. N. H.; Crossley, M. J.; Bosman, A. W.; Schenning, A. P. H. J.; Meijer, E. W. *J. Phys. Chem. B* **2000**, *104*, 2596−2606.
(27) Tsuda, K.; Dol, G. C.; Gensch, T.; Hofkens, J.; Latterini, L.; Weener, J. W.; Meijer, E. W.; De Schryver, F. C. *J. Am. Chem. Soc.* **2000**, *122*, 3445−3452.
(28) Schenning, A. P. H. J.; Peeters, E.; Meijer, E. W. *J. Am. Chem. Soc.* **2000**, *122*, 4489−4495.
(29) Adronov, A.; Gilat, S. L.; Fréchet, J. M. J.; Ohta, K.; Neuwahl, F. V. R.; Fleming, G. R. *J. Am. Chem. Soc.* **2000**, *122*, 1175−1185.
(30) Gilat, S. L.; Adronov, A.; Fréchet, J. M. J. *Angew. Chem., Int. Ed. Engl.* **1999**, *38*, 1422−1427.
(31) Birks, J. B. *Photophysics of Aromatic Molecules*; Wiley: New York, 1970.
(32) Dong, D. C.; Winnik, M. A. *Can. J. Chem.* **1984**, *62*, 2560−2565.
(33) Castanheira, E. M. S.; Martinho, J. M. G. *J. Photochem. Photobiol. A: Chem.* **1994**, *80*, 151−156.
(34) Mizusaki, M.; Kopek, N.; Morishima, Y.; Winnik, F. M. *Langmuir* **1999**, *15*, 8090−8099.
(35) Winnik, F. M. *Macromolecules* **1987**, *20*, 2745−2750.
(36) Winnik, F. M.; Winnik, M. A.; Tazuke, S.; Ober, C. K. *Macromolecules* **1987**, *20*, 38−44.
(37) Winnik, F. M. *Macromolecules* **1989**, *22*, 734−742.
(38) Winnik, F. M. *Chem. Rev.* **1993**, *93*, 587−614.
(39) Winnik, M. A.; Bystryak, S. M.; Liu, Z.; Siddiqui, J. *Macromolecules* **1998**, *31*, 6855−6864.
(40) Pranis, R. A.; Klotz, I. M. *Biopolymers* **1977**, *16*, 299−316.
(41) Arora, K. S.; Overberger, C. G. *J. Polym. Sci., Part B: Polym. Phys.* **1986**, *24*, 2275−2292.
(42) Pistolis, G.; Malliaris, A.; Paleos, C. M.; Tsiourvas, D. *Langmuir* **1997**, *13*, 5870−5875.
(43) Sideratou, Z.; Tsiourvas, D.; Paleos, C. M. *Langmuir* **2000**, *16*, 1766−1769.
(44) Pistolis, G.; Malliaris, A.; Tsiourvas, D.; Paleos, C. M. *Chem. Eur. J.* **1999**, *5*, 1440−1444.
(45) Stewart, G. M.; Fox, M. A. *J. Am. Chem. Soc.* **1996**, *118*, 4354−4360.
(46) Wilken, R.; Adams, J. *Macromol. Rapid Commun.* **1997**, *18*, 659−665.
(47) Vitukhnovsky, A. G.; Sluch, M. I.; Krasovskii, V. G.; Muzafarov, A. M. *Synth. Met.* **1997**, *91*, 375−377.
(48) Sluch, M. I.; Scheblykin, I. G.; Varnavsky, O. P.; Vitukhnovsky, A. G.; Krasovskii, V. G.; Gorbatsevich, O. B.; Muzafarov, A. M. *J. Lumin.* **1998**, *76*&*77*, 246−251.
(49) Swallen, S. F.; Zhu, Z.; Moore, J. S.; Kopelman, R. *J. Phys. Chem. B* **2000**, *104*, 3988−3955.
(50) Breslow, R.; Dong, S. D. *Chem. Rev.* **1998**, *98*, 1997−2011.
(51) Breslow, R.; Schmuck, C. *J. Am. Chem. Soc.* **1996**, *118*, 6601−6605.
(52) Hengge, A. C.; Cleland, W. W. *J. Org. Chem.* **1991**, *56*, 1972−1974.
(53) Koike, T.; Inoue, M.; Kimua, E.; Shiro, M. *J. Am. Chem. Soc.* **1996**, *118*, 3091−3099.
(54) Nango, M.; Klotz, I. M. *J. Polym. Sci., Polym. Chem. Ed.* **1978**, *16*, 1265−1273.
(55) Overberger, C. G.; Salamone, J. C. *Acc. Chem. Res.* **1969**, *2*, 217−224.
(56) Kim, N.; Suh, J. *J. Org. Chem.* **1994**, *59*, 1561−1571.
(57) Cavallo, L.; Fraternali, F. *Chem. Eur. J.* **1998**, *4*, 927−934.
(58) Scherrenberg, R.; Coussens, B.; van Vliet, P.; Edouard, G.; Brackman, J.; de Brabander, E.; Mortensen, K. *Macromolecules* **1998**, *31*, 456−461.
(59) Miklis, P.; Çağin, T.; Goddard, W. A. *J. Am. Chem. Soc.* **1997**, *119*, 7458−7462.
(60) Murat, M.; Grest, G. S. *Macromolecules* **1996**, *29*, 1278−1285.
(61) Mayo, S. L.; Olafson, B. D.; Goddard, W. A. *J. Phys. Chem.* **1990**, *94*, 8897−8909.
(62) Cuadrado, I.; Morán, M.; Casado, C. M.; Alonso, B.; Lobete, F.; García, B.; Ibisate, M.; Losada, J. *Organometallics* **1996**, *15*, 5278−5280.
(63) Chai, M.; Niu, Y.; Youngs, W. J.; Rinaldi, P. L. *Macromolecules*, in press.
(64) Bosman, A. W.; Bruining, M. J.; Kooijman, H.; Spek, A. L.; Janssen, R. A. J.; Meijer, E. W. *J. Am. Chem. Soc.* **1998**, *120*, 8547−8548.
(65) Pan, Y.; Ford, W. T. *Macromolecules* **2000**, *33*, 3731−3738.
(66) Pyrene dendrimers were very soluble in dichloromethane and chloroform, but the use of halogenated solvents in conjunction with UV excitation leads to photodegredation of pyrene.
(67) The surface densities of terminal groups were calculated by assuming that the dendrimers are spheriods having the calculated radii shown in Table 1.
(68) Goodpaster, J. V.; McGuffin, V. L. *Anal. Chem.* **2000**, *75*, 1072−1077.
(69) Previous experiments in aqueous solution have demonstrated that PPI−$(NH_2)_8$ and PPI−$(NH_2)_{64}$ yield very similar titration curves. (See: van Duijvenbode, R. C.; Borkovec, M.; Koper, G. J. M. *Polymer* **1998**, *39*, 2657−2664.) Because the total tertiary amine concentrations are comparable for the data shown in Figure 5 (1.23×10^{-6} and 1.55×10^{-6} M for PPI−Py_8 and PPI−Py_{64}, respectively), the extent of dendrimer protonation should also be comparable.

MA001379C